UHASSELT
KNOWLEDGE IN ACTION

Maastricht University

Faculty of Medicine and Life Sciences
School for Life Sciences
Master of Biomedical Sciences

Master's thesis

Early-life exposure to airborne nanoparticles and the consequences for the neurodevelopment of mice

Maartje Vangeneugden

Thesis presented in fulfillment of the requirements for the degree of Master of Biomedical Sciences, specialization Environmental Health Sciences

SUPERVISOR :

Prof. dr. Michelle PLUSQUIN

MENTOR :

De heer Kenneth VANBRABANT

2021
2022

Transnational University Limburg is a unique collaboration of two universities in two countries: the University of Hasselt and Maastricht University.

UHASSELT
KNOWLEDGE IN ACTION

www.uhasselt.be
Universiteit Hasselt
Campus Hasselt:
Martelarenlaan 42 | 3500 Hasselt
Campus Diepenbeek:
Agoralaan Gebouw D | 3590 Diepenbeek

Maastricht University

Faculty of Medicine and Life Sciences
School for Life Sciences
Master of Biomedical Sciences

Master's thesis

Early-life exposure to airborne nanoparticles and the consequences for the neurodevelopment of mice

Maartje Vangeneugden

Thesis presented in fulfillment of the requirements for the degree of Master of Biomedical Sciences, specialization Environmental Health Sciences

SUPERVISOR :

Prof. dr. Michelle PLUSQUIN

MENTOR :

De heer Kenneth VANBRABANT

Early-life exposure to airborne nanoparticles and the consequences for the neurodevelopment of mice

Maartje Vangeneugden[1], Kenneth Vanbrabant[2], Leen Rasking[2] and Michelle Plusquin[2]

[1]Student Environment Health Sciences, Hasselt University, Diepenbeek, Belgium
[2]Centre for Environmental Sciences, Hasselt University,
Agoralaan Building D - 3590 Diepenbeek, Belgium

Running title: *Neurobiological effects of airborne nanoparticles*

To whom correspondence should be addressed: Michelle Plusquin, Tel: +32 (11) 26 82 89; Email: michelle.plusquin@uhasselt.be

Keywords: Ultrafine particulate matter (< 100 nm), prenatal and early-postnatal exposure, brain, particle translocation, behavioral development, microglia and astrocyte activation, IBA-1, GFAP, C57BL/6 mice

ABSTRACT

A considering body of evidence has been published on early-life exposure to particulate matter (PM) and its impact on neurodevelopment. While particle transfer into the brain by inhalation is known to occur, this route of exposure and its associated neurotoxic effects remain largely unexplored for prenatal life. Moreover, most research has been devoted to the micro-sized PM, while nano-sized particles are considered the most toxic. This mice study set out to examine the transfer of carbon nanoparticles (CNP), a surrogate of ultrafine PM, into the brain after prenatal and/or early postnatal whole body exposure, using white-light generation under femtosecond pulsed illumination. CNP loads were measured in the brains of C57BL/6 mice, with average log (SD) counts of 0.34 (0.06), 0.38 (0.17), 0.45 (0.09), and 0.42 (0.19) particles per mm^3 tissue for sham, prenatal, postnatal and pre- and postnatal exposed mice. Nonetheless, particle loads did not differ significantly depending on condition. Furthermore, exposed offspring displayed altered behavior compared to sham-mice in the open field test, with postnatally exposed mice that spent decreased time in the open field ((W(3.000, 16.44) = 5.987, p = 0.0059) and periphery (F = 84.37, p < 0.0001). Here, the presence of CNPs in brains of pre and postnatal exposed mice was demonstrated in relation to altered behavior in the open field test. These findings suggest a direct particle transfer to the fetal brain that may contribute to negative neurological effects from early life and onwards.

INTRODUCTION

Air pollution is one of the most significant and prevalent environmental risks to human health (1, 2). The World Health Organization (WHO) has estimated that in 2019, 99% of the world population was living in areas where WHO air quality guidelines levels were not met (3). Furthermore, in 2016, outdoor pollution in rural and urban areas was estimated to contribute to 4.2 million premature deaths globally per year (3), with causes ranging from respiratory diseases (e.g., chronic obstructive pulmonary disease and pneumonia) to cardiovascular defects and stroke (4-7). Ambient air pollution majorly consists of gases such as ozone (O_3), sulfur dioxide (SO_2), nitrogen dioxide (NO_2), and carbon monoxide (CO), along with particulate matter (PM) (8). PM is the complex mixture of liquid and solid particles suspended in the air that may contain compounds from the earth's crust, elemental carbon, inorganic ions, metals, and organic compounds (9). Depending on its emission source and atmospheric processing, PM exists in various sizes, chemical compositions, surface areas, and masses (9, 10). All of these and many other physicochemical characteristics play a crucial role in the consequent health impacts of PM (11). For convenience, however, the aerodynamic diameter is most often employed to categorize the particles, ranging from coarse (PM_{10}; diameter ≤ 10

microns) to fine particles ($PM_{2.5;}$ diameter ≤ 2.5 microns) and ultrafine particles ($PM_{0.1}$ or $UFP_{;}$ diameter ≤ 0.1 microns or 100 nm). The UFPs are of most concern for human health, owing to i) their greater capacity to deposit in the lower respiratory tract and consequently travel through the circulation to distant organs (12, 13) and ii) their strong tendency to adsorb other toxic compounds (e.g., polycyclic aromatic hydrocarbons (PAHs) and benzene) resulting from their high surface-to-volume ratio (14, 15). Outdoor UFPs are mainly combustion-derived (i.e., by burning fuels) and carbonaceous of nature originating from traffic and industries (e.g., soot) (16). They are composed of an elemental carbon core encompassed by organic carbon and minor portions of metals, nitrate, and sulfate compounds (17).

A critical target of UFPs that goes beyond the lungs is the brain. Adverse effects are either exerted indirectly by inducing systemic inflammation or directly by particles entering the brain (18). The direct way is enabled by two main exposure routes. First, inhaled UFPs may enter the circulation by crossing the alveolar-capillary barrier, through which they may further travel toward the brain (19). Even though the central nervous system (CNS) is well isolated from the circulation by the tight blood-brain barrier (BBB), blood-derived particles have been shown to breach this protective layer rendering it even more permeable (20). The second and probably the most prevailing route for particle uptake occurs via the olfactory region (21). Upon inhalation, UFPs can penetrate the olfactory epithelium through the oral or nasal cavity, eventually reaching the olfactory bulb (22). From there on, they can further move into different brain areas, such as the hippocampus (19). Within 4-24h after inhalation, UFPs could already be detected in the brain (22).

Over the last decades, extensive research has been conducted to understand better the neurotoxicity behind inhaled particle exposure (23). An escalating body of evidence has associated exposure to PM with poor brain outcomes and a higher incidence of neurological diseases (24). For example, animal and human studies indicated a link between $PM_{2.5}$ exposure and decreased cognitive functions (25-27). Moreover, long-term exposure to $PM_{2.5}$ has been correlated with a significant increase in risk for depression (28, 29). Recently, several studies proposed evidence suggesting that general PM exposure may contribute to the incidence or worsening of neurodegenerative diseases, such as dementia (30, 31), Alzheimer's disease (31, 32), Parkinson's disease (33), and multiple sclerosis (34). Notably, none of these studies investigated the contribution of UFPs as a separate category to these outcomes, rendering it challenging to assess whether effects were manifested by UFPs. Reasons for the limited number of studies concerning UFPs may be the lack of standard measurement techniques and personalized data (35, 36), underscoring the need for further research.

Particularly susceptible to toxic compounds such as PM are pregnant women, their growing fetuses, and young children (37). It is already widely acknowledged that prenatal exposure to $PM_{2.5}$ is linked to an increased risk of preterm delivery and low birth weight (38, 39). Several factors contribute to this increased health risk. First of all, the oxygen consumption and ventilation of the mother are greatly increased during the pregnancy (40), leading to higher particle intakes as compared to a non-pregnant person. Second, all of the organs and body systems of the fetus are forming entirely, and any harm at that stage may result in life-long consequences (41). Third, the metabolism and immune system during fetal life and childhood are still too immature to efficiently detoxify and eliminate unwanted substances (42). Finally, children generally have higher breathing rates than adults and given their height, they are also closer to the ground where e.g., exhaust particles from cars are emitted (37).

Chronic and acute exposure to PM during crucial periods of perinatal life may also affect the neurodevelopmental trajectory. Numerous human and rodent studies have explored the impact of pre- and early-postnatal exposure to PM, delivering strong evidence for links with altered brain functions and behavior (43-45). Examples of altered performance measures are reduced working memory (46), learning (47, 48), cognition (46), reaction times (49), attentiveness (49), along with altered behavioral regulation (50). Additionally, mood disorders have been observed in several rodent studies following early-life exposure to PM,

including symptoms of depression and anxiety (51, 52). In a recent study by our research group, black carbon particles were identified on the fetal side of human placentae providing evidence that direct exposure of the fetus to PM is possible (53). In summary, pre- and early-postnatal exposure to PM may affect the brain both directly and indirectly, which may result in neurodevelopmental delay and disturbances. Consequently, this may sensitize the infant to develop chronic neurological diseases later in life, as described by the Developmental Origins of Health and Disease hypothesis (54).

Several cellular mechanisms have been put forward that may underlie or contribute to these negative effects on the CNS. Examples include mitochondrial dysfunction (55), endoplasmic reticular stress (56), DNA adduct formation (57), and disturbance of protein homeostasis (58). However, the most commonly described effects are induced oxidative stress and neuroinflammation (58), closely intertwined mechanisms involved in neurodegeneration (59). Growing evidence implicates the involvement of glial cells in neuroinflammation from air pollution exposure (60). Glial cells are the non-neuronal cells of the CNS (including oligodendrocytes, astrocytes, and microglia) comprising 80% of the human brain (61). They are highly sensitive to systemic inflammation and external stimuli entering the brain, such as UFPs. PM exposure experiments with rodents have shown that astrocyte and microglia numbers increase significantly after exposure, specifically in the dentate gyrus, hippocampus and cortex. This phenomenon, called glial cell activation, is part of an inflammatory response elicited by the astrocytes and microglia in response to the exogenous particles (62).

Over the past decades, extensive research has been carried out to understand better the adverse effects of pre- and early postnatal exposure to PM on the brain. However, limited studies have explored the respective contribution of UFPs to these consequences, while this size fraction is considered the most hazardous. Furthermore, it remains unclear whether the impact of pre- and early-postnatal exposure differs for the CNS, as most studies focus on either one of the exposure periods. Here, these knowledge gaps were addressed by exposing mice whole body, pre- and postnatally to spark-generated carbon nanoparticles (CNPs; 1-20 nm in diameter). CNPs represent a relevant toxicological surrogate from diesel engines as they constitute the core of combustion-derived particles (63). Even though engineered CNPs may possess different properties, it is highly plausible that they share modes of action with combustion-derived UFPs. The hypothesis was that prenatal exposure to CNPs during critical developmental stages of pregnancy in mice will adversely affect offspring's neurological reflexes, with a larger impact of postnatal exposure, and that this is mediated by glial cell activation. To approach this hypothesis, we investigated the particle transfer toward the brain using our in-house measuring method based on the generation of white-light on the non-incandescence-related white light generation of particles under femtosecond pulsed illumination. This allows us to determine personalized exposures for each mouse. Additionally, we evaluated offspring's behavioral development and performance in the homing and open field tests. Lastly, we aimed to explore glialcell activation in the offspring brains to gain mechanist insights. Together with previous research, our study can provide substantial new knowledge on the effects of early-life exposure on neurodevelopment of mice.

EXPERIMENTAL PROCEDURES

1. Illustration of particle transfer into the brain

Brains of 18 female NMRI mice were provided for this study by Hougaard K.S. *et al.* from the department of Public Health, Environmental Health at the University of Copenhagen. All experimental and ethical procedures are described in detail by Skovmand *et al*. (64) (ethical permit no. 2015-15-0201-00569). Briefly, mice were exposed whole body to either HEPA-filtered air (sham n = 6) or to target Printex 90 concentrations of 4.6 and 37 mg/m^3 (low n = 6, high n = 6, respectively) for 45 min/day over 15 consecutive days. Animals were euthanized 26-28 days after concluding the exposures, and brains were isolated and stored at -80°C. Sample processing for the detection of carbon black particles occurred as described in "Particle detection in brains".

2. Study towards early-life exposure to CNPs

Animals – Mice from the C57BL/6J OlaHsd strain were purchased at 5 weeks of age from Envigo (The Netherlands) and randomly assigned to individually-ventilated cages (GM500 Mouse IVC Green Line, Tecniplast, UK) holding 5 females each; males were housed individually. All animals were kept in a temperature-controlled environment (21-23°C), having *ad libitum* access to a standard diet and water in their home cage under a reversed 12h light/dark cycle (4.00h – 16.00h). At 16 weeks, mice time-mated (designated gestational day (GD) 0), and pregnancy was confirmed on GD 8 by a weight gain of 0.7 up to 3.5 g. All procedures were conducted according to EU Directive 2010/63/EU for animal experiments and approved by the Local Ethical Committee for Animal Experimentation (Hasselt University, Diepenbeek, Belgium; ID 202148B and 201864A1).

Exposure – The pregnant dams were exposed whole body over GD 8, 9, 16, and 17 for 4 h/day, to either HEPA-filtered clean air or target CNP concentrations of 440 μg/m^3. No food and water were provided to avoid oral particle intake. Clinical signs were assessed 4 times and mice were returned to their home cage after the exposure. Birth was expected on GD 20, and designated postnatal day (PND) 0. Offspring (n = 165) were randomly divided to receive an additional postnatal exposure in the same conditions as previously over PND 4-7 and 10-13. A total of 4 offspring groups was established, in the following referred to as the sham (control, n = 37), prenatal (n = 44), postnatal (n = 41), and pre and postnatal group (n = 43). A schematic illustration of the experimental timeline is shown in Figure 1. During the exposure, the mice were held in separate wire mesh cages (26 x 15.5 x 18 cm) inside a temperature-controlled 200L inhalation unit (85 x 64 x 37 cm), designed to deliver an evenly distributed exposure. Electric discharge particle generators (VSP-G1, VSPARTICLE, The Netherlands) were employed to generate an aerosol of nanoparticles from carbon electrodes through which 8 L/min nitrogen was flown. The output was mixed with 2.2 L/min oxygen and 10 L/min filtered, moisturized room air, which was directed to the exposure units. More information regarding exposure characterization and monitoring can be found in the supplementary information.

Behavioral testing – For all tests, a max. of one pup per sex per litter was included to minimize litter effects. Animals across different conditions were tested in a random order and the observer, who was blinded to the exposure status, performed most tests. Behavioral development was evaluated on PND 16 in the light period by tests for righting, negative geotaxis and cliff drop avoidance reflexes. Scoring was based on quantitative measurements and predetermined criteria (more details in the supplementary information). Mice were max. 20 min removed from their mother and held on heating pillows as long as possible.

Homing (PND 19) and open field (PND 21) tests were executed in the dark phase and used to evaluate olfactory discrimination performance, and locomotor activity and exploring behavior, respectively. Mice were transferred to a clean, empty cage ± 18 min prior to testing. In the homing test, animals were left to choose between 0.5 g of home cage or clean bedding in 90 x 15 mm petri dishes (one for each bedding material) placed in the left and right zone of a rectangular arena (42.5 x 26.5 cm). The position of the home cage bedding was alternated each trial. Trials commenced in the center of the arena and the animal was video recorded for 5 min. EthoVision XT software (Noldus Information Technology, The Netherlands) tracked the total distance moved (cm), velocity (cm/s), and the duration (s) in the left and right zones. For the open field test, mice were treated identically before onset of the tests. Exploring behavior and locomotion was assessed for 15 min in a squared open field (50 x 50 cm) Locomotion was tracked using the same software, and total distance moved (cm), mean velocity (cm/s), duration (s) in the center, periphery and borders, as well as the number of visits to each zone, were registered.

Particle detection in brains – At PND 14, 18 offspring mice (n=4 sham; n=5 prenatal; n=4 postnatal; n=5 pre and postnatal) were anesthetized with pentobarbital (200 mg/kg; i.p.) and transcardially perfused using Ringer solution. Right brain hemispheres were fixed in 4% paraformaldehyde for 24h, cryopreserved in a 15-30% sucrose gradient solution for a minimum of 3-

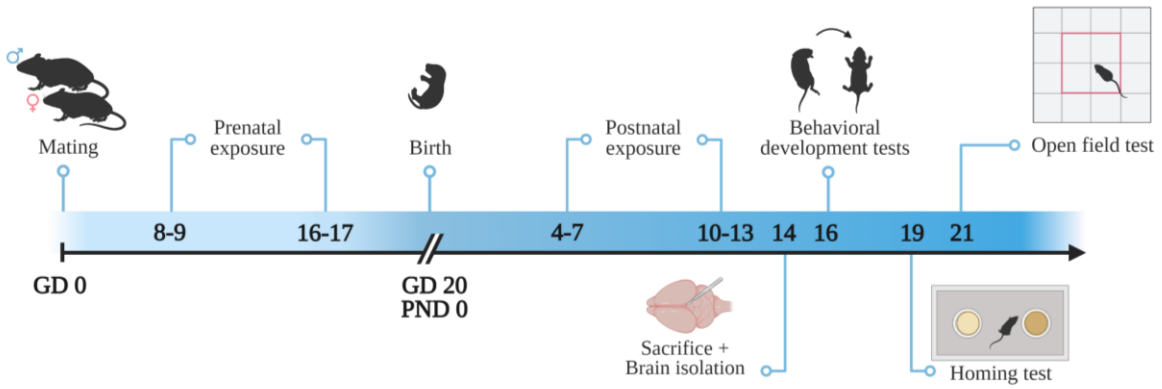

Figure 1 Schematic illustration of the experimental timeline. The numbers represent the days and day of mating is designated GD 0. On GD 8, 9, 16, and 17, a prenatal exposure to either HEPA-filtered air (0 µg/m^3) or aerosolized CNPs (440 µg/m^3) was delivered through maternal whole-body inhalation. Birth was expected at GD 20, indicated by the slashes, and designated PND 0. An additional postnatal exposure was delivered to the offspring at PND 4-7 and 10-13, again to either HEPA-filtered air (0 µg/m^3) or aerosolized CNPs (440 µg/m^3), resulting in 4 different offspring conditions: sham, prenatal, postnatal, and pre and postnatal exposed mice. Part of the offspring was sacrificed at PND 14 to isolate the brains for particle analyses. The other offspring mice were subjected to behavioral tests at PND 16, including for righting, negative geotaxis, and cliff aversion. On PND 19 and 21, the homing and open field tests were performed, resp. Abbreviations: GD = gestational day, PND = postnatal day, CNP = carbon nanoparticle.

6h and 12h, respectively, and embedded in OCT compound.

Using a cryostat CM3050 S (Leica Biosystems Inc., USA), 20 µm sections were cut and mounted onto glass slides. Particles in the brain sections were detected employing our specific in-house technique based on the non-incandescence-related white light generation of particles under femtosecond pulsed illumination as described by Bové *et al.* (65). Brain images were obtained at room temperature using a Zeiss LSM 510 (Carl Zeiss, DE) and femtosecond pulsed laser (150 fs, 810 nm, 80 MHz, MaiTai DeepSee, Spectra-Physics, USA) set to a wavelength of 810 nm using an EC Plan-Neofluar 10x/0.30 objective (Carl Zeiss, DE). The 2x2 tile scans of brain sections were collected with a 1754.86 µm pixel size and 2.51 µsec pixel dwell time. Per sample, 10 brain sections in total were recorded and acquired using ZEN Black 2.0 software (Carl Zeiss, Germany). To count the number of CNPs in the obtained tile scans, a customized MATLAB program (MATLAB 2010, MathWorks, The Netherlands) was used. Lastly, the counts were averaged and normalized to the brain area using Fiji (ImageJ v2.0, Open source software) and expressed as the number of particles found per mm^3.

Immunofluorescence – Two brain sections per offspring condition were stained for GFAP (glial fibrillary acidic protein) and IBA-1 (ionized calcium-binding adaptor protein-1), which are markers for astrocyte and microglia activation, respectively. Non-specific binding sites were blocked with protein block (C0909, Agilent Dako, USA) for 60 min; tissue sections were probed with rabbit polyclonal antibody against mouse GFAP (1:1000, HPA056030, Sigma Aldrich, Germany) or rabbit polyclonal antibody against mouse IBA-1 (1:1000, 019-19741, FUJIFILM Wako Chemical Corporation, USA) overnight at 4°C in a humid chamber. After washing, tissue sections were incubated with an Alexa Fluor® 488 conjugated goat-anti rabbit secondary antibody (1:1000, A11008/A11006, Invitrogen, USA). All antibodies were diluted in 10% protein block/PBS. SYTO™ 61 Red (1:750, S11343, Invitrogen, USA) was used as a nuclear counterstain. Tile scans of 2x2 images of stained tissue sections were acquired within the cerebrum and cerebellum of each stained sample using a Zeiss LSM 880 (Carl Zeiss, DE) in the setup as described before, now also using a Plan-Apochromat 20×/0.8 (Carl Zeiss, Germany) objective resulting in a field of view of 9000 x 9000 µm^2 with a 0.83 x 0.83 µm^2 pixel size and a pixel dwell time of 2.51 µs. Alexa Fluor® 488-labeled microglia and astrocytes, and SYTO™ 61 Red-

labeled nuclei were excited by a 0.64 mW 488 He–Ne laser and a 5 mW 633 He–Ne laser, respectively. Band-pass filters of 400-410 nm and 450-650 nm were used to filter the emission signal from the labeled glial cells and nuclei. More information regarding quantification of immunofluorescent staining can be found in the supplementary information.

Statistical analysis – Statistical analysis was carried out using commercially available GraphPad Prism software (GraphPad Prism 8, GraphPad Software Inc., USA). *P*-values < 0.05 were considered statistically significant. In general, ordinary one-way ANOVA was employed to compare means (SD) across conditions, followed by post-Tukey or Games-Howell's multiple comparison tests. Outliers were removed by ROUT analyses (Q = 1%). Assumptions for normality and equal variance were assessed by the D'Agostino-Pearson normality test and Brown-Forsythe test for heteroscedasticity. In case assumptions were violated, first a log transformation was executed. If assumptions were still not met, a Welch's ANOVA or non-parametric Kruskal-Wallis test was executed.

RESULTS

1. Illustration of particle transfer into the brain

To confirm the ability of carbonaceous particles to reach the brain after inhalation, brain tissues of 18 mice with either a sham (n = 6; 0 mg/m^3), low (n = 6; 4.6 mg/m^3) or high (n = 6; 37 mg/m^3) exposure to Printex 90 (carbon black; CB) were screened for their CB load (Figure 2). All the screened brain samples contained CB particles, with an average log (SD) particle count 0.27 (0.10), 0.31 (0.07), and 0.36 (0.15) particles per mm^3 tissue for sham, low, and high exposed mice, respectively. Despite the different deposited doses, the differences among the means were negligibly small and not significant (W = 0.1896, p = 0.8306).

2. Study towards early-life exposure to CNPs

CNP load in brains of offspring – To compare the particle transfer to the brain after pre- and/or postnatal exposure, brain tissues of 18 mice with either a sham (n = 4; 0 µg/m^3), prenatal (n = 5; 440 µg/m^3), postnatal (n = 4; 440 µg/m^3) or pre and postnatal (n = 5; 440 µg/m^3) exposure were screened for their CNP load. All the screened brain samples contained CNPs, with an average log (SD) particle count of 0.34 (0.06), 0.38 (0.17), 0.45 (0.09), and 0.42 (0.19) particles per mm^3 tissue for sham, prenatal, postnatal and pre and postnatal exposed mice. As can be seen from Figure 3, there were some slight differences in particle load with the highest levels detected in brains of mice with an additional postnatal exposure administration. However, a one-way ANOVA revealed that these differences were not significant (F = 0.2210, p = 0.8802).

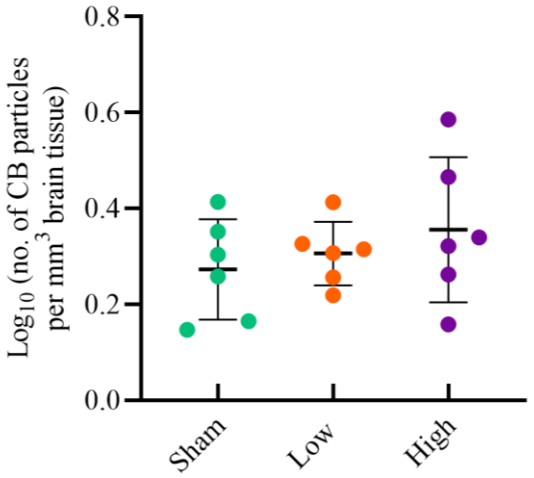

Figure 2 Scatter dot plot showing the CB loads found in 18 mice brains across the 3 exposure conditions. Green, orange and purple dots indicate sham (n = 6; 0 mg/m3), low (n = 6 n = 6; 4.6 mg/m3) and high (n = 6; 37 mg/m3) exposed mice, respectively. CB loads were measured in a region of a 3x3 image, repeated within 10 different sections per brain sample. Number of particles per mm^3 tissue were log transformed. The bars represent the mean ± SD. An ordinary one-way ANOVA (α = 0.05) was performed.

Effects on behavioral development – The impacts of the different early-life exposures to CNPs on neurodevelopment were assessed by evaluating offspring's behavioral development at PND 16. An overview of the results is provided in Figure 4. The data was not separated by sex since it only explained ± 0.87 % of the total variance. The first test examined the righting response requiring vestibular cues and motor ability to return onto the

paws. Figure 4A demonstrates the mean duration needed to right 180° across the 4 conditions., which ranged from 4.82 (postnatal group) to 5.96 (prenatal group) seconds; no difference greater than 0.13 seconds was observed which is negligibly small ($F = 0.1953$, $p = 0.8989$).

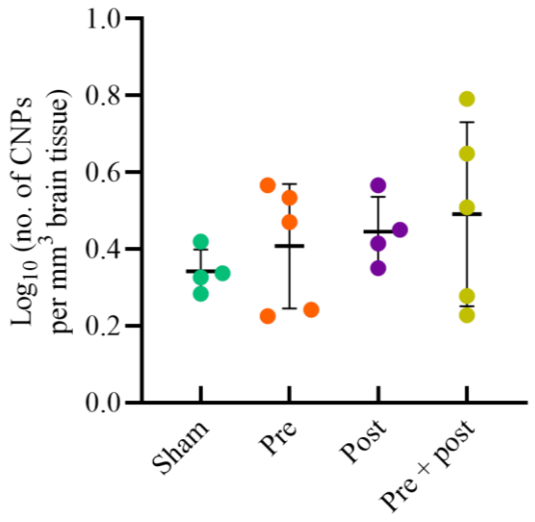

Figure 3 Scatter dot plot showing the CNP loads found in 18 mice brains across the 4 exposure conditions. Green, orange, purple, and yellow dots indicate sham ($n = 4$), prenatal ($n = 5$), postnatal ($n = 4$), and pre and postnatal ($n = 5$) exposed mice, respectively. CNP loads were measured in a region of a 3x3 image within 10 different sections per brain sample. Number of particles per mm^3 tissue were log transformed and are presented as means. Group means are marked by the horizontal lines. The error bars represent the SD. A one-way ANOVA ($\alpha = 0.05$) was performed.

Next, the negative geotaxis test was performed to further assess motor coordination and vestibular cues, which entails the upward reorientation and climbing performance of the pup placed face down on a slope. Overall, mice showed a comparable amount of time to complete the negative geotaxis response, and differences did not differ statistically (Figure 4B) ($F = 0.65$, $p = 0.60$). This similarity in performance was also reflected by the nearly identical scores given for their negative geotaxis behavior, as presented in Figure 4C ($F = 0.32$, $p = 0.81$).

Lastly, the cliff drop avoidance test was carried out examining paw strength, motor coordination and vestibular cues in order to move away from the edge of an elevated surface (Figure 4D and E). Again, very similar response times were recorded for this reflex, with mean times ranging from 1.51 (sham group) to 2.43 (prenatal group) seconds maximum ($H = 1.09$, $df = 3$, $p = 0.78$). The difference in scores given for the cliff aversion response were also not significantly different, all approximating a value of 2 ($F = 0.91$, $p = 0.44$).

Behavior in the homing and open field test – For both tests, sex was not included as a factor as it only explained max. 3% of the total variance. The olfactory discrimination performance of offspring was evaluated on PND 19 in the homing test, as olfactory dysfunction is a known defect linked with air pollution exposure. Figure 5 provides the results obtained from comparing the left and right arena zones with either home cage or clean bedding. Overall, the mean time spent at the side of the home cage bedding was quite comparable across the conditions (Figure 5A); differences were not statistically significant ($F = 0.72$, $p = 0.55$, $R^2 = 0.06$). Mice of the prenatal group spent the most time at the home cage bedding side with an average (SD) time of 251.21 (20.77) seconds, followed by the mice of the sham and pre and postnatal group with a nearly same duration of 248.05 (14.98) and 248.38 (14.06) seconds, respectively; the lowest time was recorded in the postnatal group and was 242.48 (21.92).

Turning to the frequency or number of visits to the home cage bedding side, values generally correspond to what has been observed for the duration (Figure 5B). The prenatal group had the smallest number of visits with a mean (SD) of 11 (6.68), which is likely if the mice spend more time inside the zone instead of crossing its borders. The other groups showed a similar number of visits, ranging from 14 (SD sham= 9.55; SD pre and postnatal = 6.93) to 15 (SD postnatal = 13.96). None of these differences were statistically significant ($F = 0.34$, $p = 0.79$, $R^2 = 0.03$).

In the open field test at PND 21, exploring and anxiety-like behavior were examined. The results obtained from the open field test are set out in Figure 6. From Figure 6A, it can be interpreted that mice generally moved a similar distance; differences in mean were not considered significant ($F = 0.55$, $p = 0.65$, $R^2 = 0.04$). This data corresponds to the mean velocities recorded (Figure 6B), where groups with a slightly increased velocity

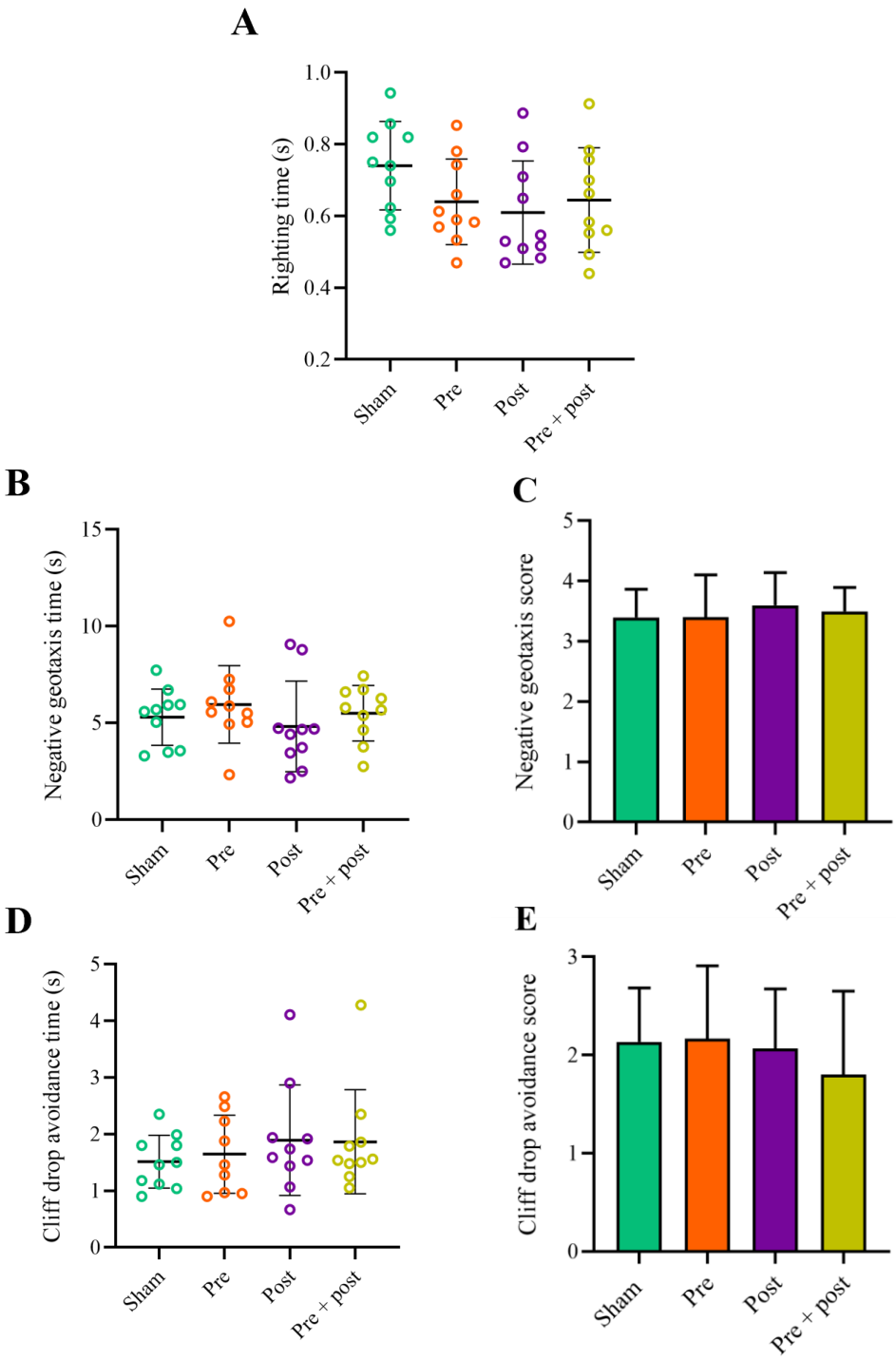

Figure 4 Scatter dot plots and bar plots showing the performance of offspring (n = 10 per group) in the behavioral developmental tests across the different conditions (green = sham group; orange = prenatal group; purple = postnatal group; yellow = pre and postnatal group) at PND 16. **A** – Time in seconds required to right through 180°. **B** – Time in seconds to turn upwards in the negative geotaxis test. **C** – Scores given for the negative geotaxis response (score 0 = falling down the slope or failing to return; score 1 = turning the head; score 2 = turning the body up 90°; score 3 = turning the body up 180°; score 4 = climbing up the slope). **D** – Time in seconds required to remove the snout and paws from the edge. **E** – Scores given for the cliff avoidance response (score 0 = remaining motionless or falling from the edge; score 1 = turning the head; score 2 = turning the head aside and pulling back the forepaws; score 3 = initiating a backward movement). The tests were repeated thrice per mouse to deliver an average time/score. Bars indicate the mean ± SD. One-way ANOVA ($\alpha = 0.05$) was employed for the data shown in A-D. Data in E was analyzed by a non-parametric Kruskal-Wallis test ($\alpha = 0.05$). n = 10 per condition.

also showed a slightly longer distance moved, and *vice versa*. Here the data was also not significantly differing (F = 0.70, p = 0.56, R^2 = 0.06), suggesting no altered exploring behavior.

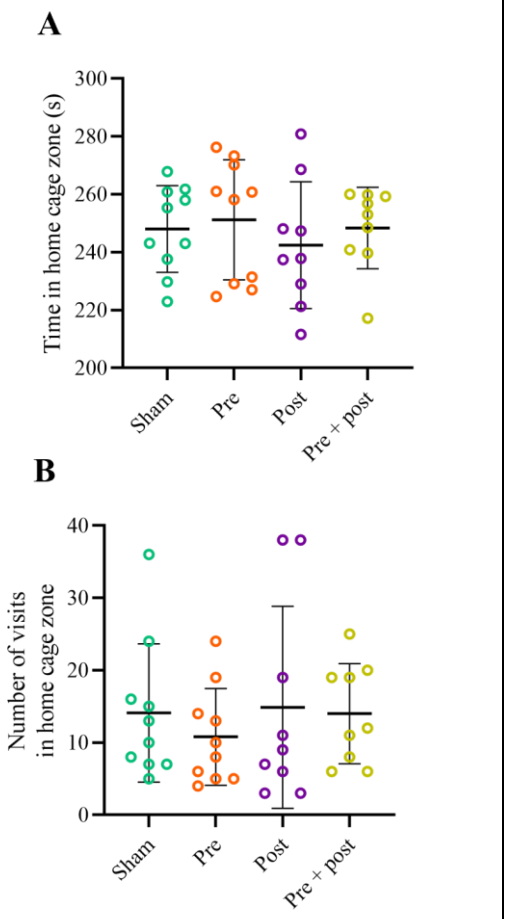

Figure 5 Scatter dot plots presenting the performance of offspring in the homing test across the different conditions (green = sham group; orange = prenatal group; purple = postnatal group; yellow = pre and postnatal group) at PND 19. **A** – Time in seconds spent in the zone with home cage bedding. **B** – The number of visits to the zone with home cage bedding. Bars indicate the mean ± SD. One-way ANOVA (α = 0.05) was employed. n = 10 per condition (1 outlier removed in postnatal condition)

Next, time spent in the center was tracked as a measure of anxiety-like behavior. In Figure 6C, there is clearly a trend of decreased time spent in the center for mice that received a postnatal exposure (regardless of prenatal exposure), with the lowest mean duration (SD) of 60.35 (13.44) seconds recorded for the postnatal group. A Welch's ANOVA confirmed a significant association between the conditions and the time in the center (W (3.000, 16.44) = 5.987, p = 0.0059). Applying the Games-Howell's multiple comparison test showed that the values of the postnatal group differed most from the sham and prenatal group, with nearly significant p-values of 0.0857 and 0.0868, respectively.

Turning to the number of visits to the center, this trend became less apparent, with mean (SD) numbers ranging from rounded 38 (8.67) for the postnatal group to 44 (24.05) , 52 (18.73) and 53 (23.65) for the pre and postnatal, sham, and prenatal group, respectively. The decreased apparency in trend was also reflected in the statistical values, where an ordinary one-way ANOVA showed decreased significance (F = 1.14, p = 0.3499, R^2 = 0.09).

Additionally, exploring in the periphery and borders of the arena was tracked to further assess anxiety-like behavior. The results, as shown in Figure 6E and F, indicate that the postnatally exposed mice spent significantly less time in the periphery and borders compared to the other conditions (F = 84.34, p < 0.0001). When turning to the number of visits to the periphery and borders, it appears that the sham group visited the periphery and borders the most, significantly differing from the values observed for the postnatal group (F = 2.823, p = 0.0497).

Immunofluorescent analyses of IBA-1 and GFAP expression in the brain – To assess whether perinatal exposure to CNPS could lead to glial cell activation, the expression of IBA-1 and GFAP was measured within the cerebrum and cerebellum of mice across the different conditions. Figure 7 shows the results of the immunofluorescent staining, including fluorescent images and scatter dot plots presenting the areas of expression per marker. It should be noted that no statistical analysis could be carried out, as the sample sizes were too low. Hence results should be interpreted with caution and only serve as a pilot experiment. Nonetheless, in all screened samples, expression of both IBA-1 and GFAP was found, with overall higher expression levels of IBA-1. Looking at the area of expression for IBA-1 positive cells (Figure 7G), increased levels were found in the postnatal group and this trend was most apparent from the cerebrum.

The pre and postnatal group showed a similar increase in IBA-1 expression for the pre and

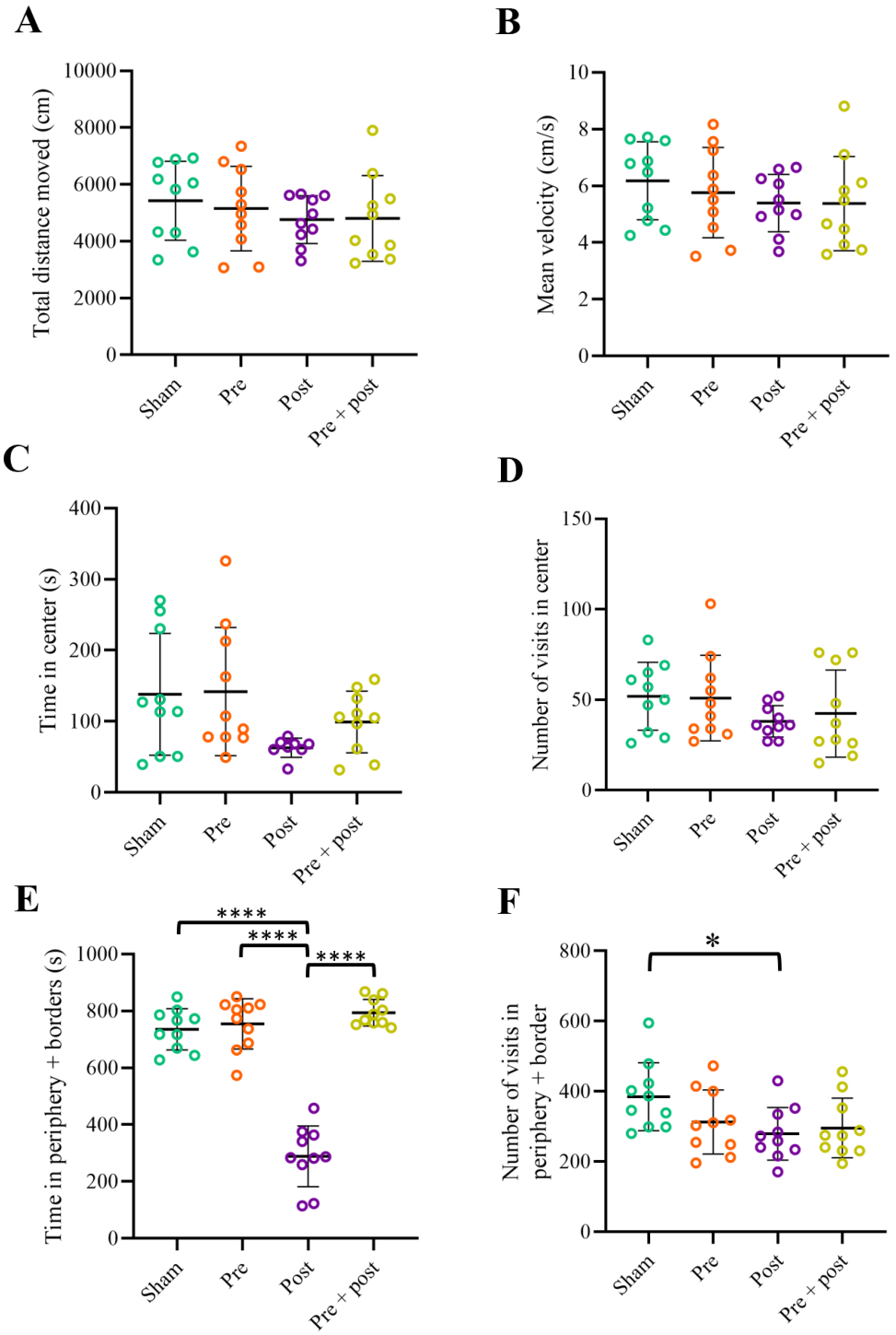

Figure 6 Scatter dot plots showing the performances of offspring (n = 10 per group) in the open field test across the different conditions (green = sham group; orange = prenatal group; purple = postnatal group; yellow = pre and postnatal group) at PND 21. **A** – Total distance moved in centimeters during the 15 min test. **B** – Mean velocity of ambulation in centimeters per second. **C** – Time in seconds spent in the center. **D** - The number of visits to the center. **E** – Time in seconds spent in the periphery and borders. **F** – Number of visits to the periphery and borders. Bars indicate the mean ± SD. Ordinary one-way ANOVA was employed for all data followed by Tukey's multiple comparison test, except for B where a Brown-Forsythe ANOVA was performed. $\alpha = 0.05$, $*p < 0.05$, $****p < 0.00005$.

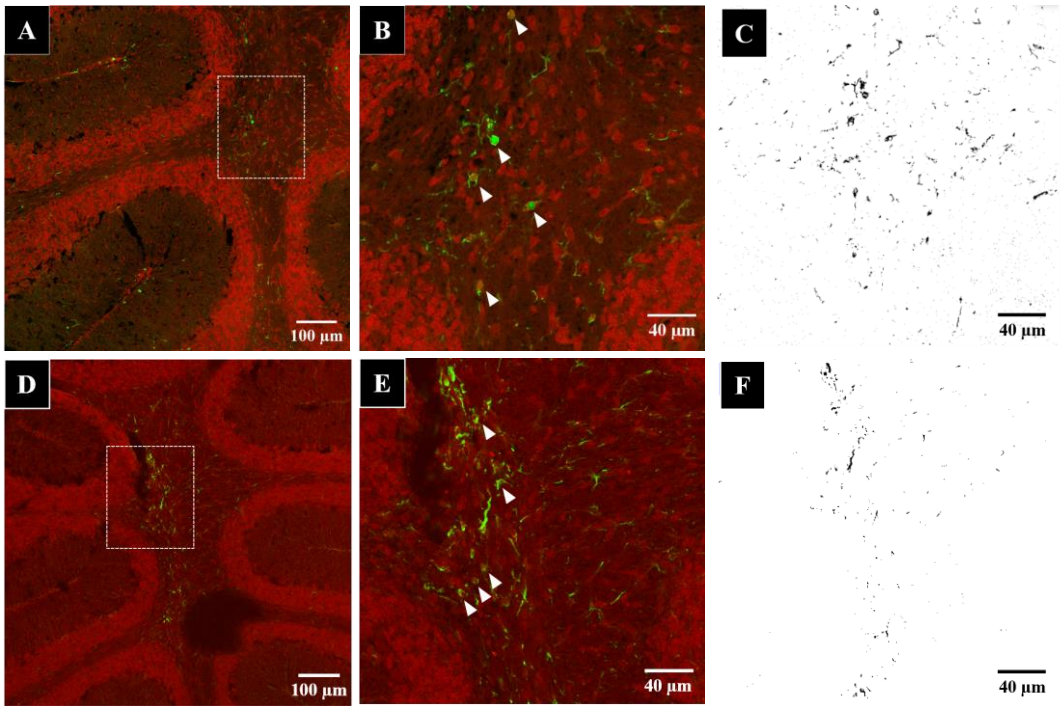

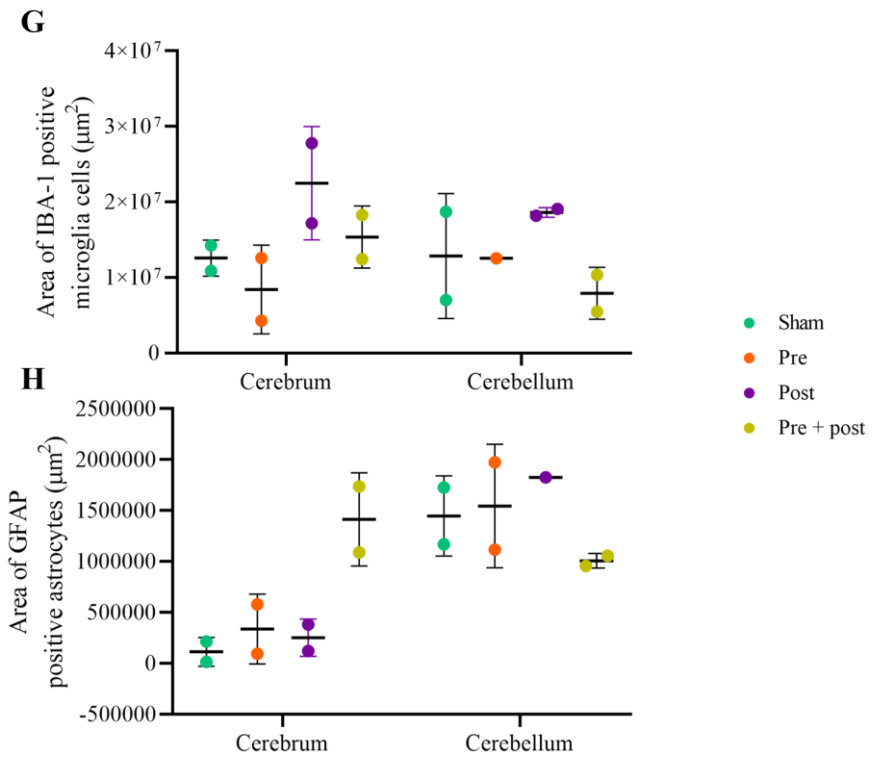

Figure 7 Immunofluorescence staining of IBA-1 and GFAP in offspring brains (n = 2 per condition) as markers for microglia and astrocyte activation, respectively. **A** and **D** – Fluorescent images (10x) of IBA-1 positive microglia cells (A, green) and GFAP-positive astrocytes (D, green) in the cerebellum of a mouse from the pre and postnatal group. Nuclei were stained with Syto-61 Red (red). **B** and **E** – Enlarged view of the panels indicated in A and D, with arrows indicating the positively stained microglia (B) and astrocytes (E). **C** and **F** – Grayscale views of B and D, respectively. Scale bar: 100 (A, D) and 40 µm (B, C, E, F). **G** and **H** – Scatter dot plots showing the areas (µm^2) of expression of IBA-1 positive microglia (G) and GFAP-positive astrocytes (H) in the cerebrum and cerebellum of offspring across the 4 conditions based on the grayscale views. One value in H (postnatal group, cerebellum) is missing because the cerebellum could not be captured. Bars indicate mean ± SD. Data was not statistically analyzed because of the low sample size.

postnatal group, especially when compared to the prenatal group. However, this difference in IBA-1 was only observed within the cerebrum.
Considering the GFAP staining (Figure 7H), a clear difference is visible in expression depending on the brain region, with the cerebellum showing higher levels of GFAP expression across all the conditions. However, within the cerebellum, there was overall no difference in GFAP expression between sham and any other exposure conditions. Albeit the lower GFAP expression within the cerebrum, levels prominently increased in the pre and postnatal group as compared to the other conditions.

DISCUSSION

This experimental study investigated the neurodevelopment of mice following early-life exposure to CNPs, a toxicological surrogate of outdoor UFPs. We were able to detect particles in the brains of offspring mice that were pre and/or postnatally exposed to concentrations of 440 µg/m^3 CNPs, by using a highly sensitive detection method based on white-light generation under femtosecond pulsed illumination. Both prenatal and postnatal exposure was associated with altered offspring behavior in the open field test.

In a study conducted with rats, polystyrene nanoparticles were detected in the brains of newborns 24h post maternal exposure to 2.64 x 10^{14} particles via intratracheal instillation on GD 19 (66). Another, more recently published research by Calderon-Garcidueñas *et al.*, found striking evidence of environmental nanoparticles in the brains of 8-12.5 weeks old human fetuses coming ambient exposure (67). Accumulation of nuclear, organelle, and cytoplasmic nanoparticles was observed in the neurons and primitive glial cells. Despite the differing nature or delivery of the nanoparticles, our study corroborates these findings, suggesting that even before birth, the brain is already subject to direct exposure of PM.

Even though particles were detected in all screened brain samples, this study has been unable to demonstrate a dose- or condition-dependent particle uptake in the adult and offspring brains. This result was somewhat unexpected, as one would assume to find a higher particle load in the brains of the high or more recently exposed postnatal groups. Such a relationship has been observed by Hameed *et al.*, where an increased uptake of PM particles in the brains of mice exposed to polluted air (70 µg/m^3 $PM_{2.5}$; 10,000-20,000 particles/m^3 $PM_{0.1}$) was measured in comparison to sham-exposed mice (68). They detected up to 4,458 particles on the surface of the brains of exposed mice, while the brains of sham-exposed mice only showed an average of 867 particles. However, it is essential to bear in mind that these mice were exposed for 8 h/day, 6 days per week, for 24 weeks, which is a much more intense exposure treatment than the current study. Hence, these findings cannot be fully extrapolated to ours.
On the other hand, it could be questioned whether the exposure in the current study was of efficient duration to lead towards a brain deposition as reported by Hameed *et al.* Another study with rats, however, revealed a significant and persistent increase of ultrafine elemental ^{13}C particles in the olfactory bulb of rats following only one inhaled exposure of 6 hours to 160 µg/m^3 ^{13}C (22). Interestingly here was that the concentrations of the deposited ^{13}C particles increased over time, from 0.35 µg/g on day 1 to 0.43 µg/g by day 7. These findings by Öberdörster *et al.* support the idea of a gradual and dose-dependent uptake of particles into the brain, at 24h following inhalation.

There are yet other explanations that may underlie this lacking relationship between condition and brain particle load. The studies above sampled the brains almost immediately to max. 7 days after the conclusion of the exposure. In contrast, in our CB pilot study (64), mice were only sacrificed a month after exposure. This delayed sampling might have led to a significant clearance of the particles over time by the microglia (79). On contrary, the brains of the perinatally exposed mice were already sampled within 24h. Hence, it might be that the particle transfer was still ongoing. Finally, it is assumed that the particle deposition occurs mostly in the olfactory bulb, while images were taken of the whole brain. This could have led to regions empty of particles, significantly decreasing the averages of particle counts. Better insights into the particle deposition and clearance time are issues for future research.

In the open field test, altered behavioral patterns were observed in association with perinatal exposure to CNPs. Postnatal exposure resulted in decreased activity in both the center and periphery. At first side, this appears somewhat unexpected as one would expect that decreased activity in the center is associated with the opposite behavior in the periphery. However, stratifying the duration by border and periphery as separate areas showed a clear trend of the postnatal group spending the most time in the borders, specifically. This behavioral pattern is termed thigmotaxis (i.e., to stay close to walls when exploring an open space), which is a well-established indicator of animal fear (69). It can therefore be postulated that postnatal exposure to CNPs resulted in anxiety-like behavior. Several previous studies documented an association between air pollution/PM and anxiety, both in rodents and humans. Neonatal rats intranasally exposed to $PM_{2.5}$ (2 or 10 mg/kg body weight, PND 3-15), for instance, showed a dose-dependent increase in anxiety-like behavior in the elevated plus maze at PND 28 (i.e., another animal test to explore anxious behavior) (70). In a children's cohort research, exposure to traffic-related air pollution during early-life was significantly associated with anxiety symptoms in 12-year-old children (71), supporting the findings of the *in vivo* animal studies. Several suggestions have been made to explain this link between air pollution and anxiety. Power *et al.* proposed that inflammation and oxidative stress induced by PM, may trigger or exacerbate anxiety symptoms. This hypothesis is based on the simultaneous observation of anxiety-related behavior and oxidative stress in the brains of rodents (72-74). Furthermore, neurotransmitter signaling pathways seem to be a potential target of PM (75). Early-life exposure to diluted diesel exhaust (171 $\mu g/m^3$, 8 h/day, GD 2-16) resulted in altered levels of dopamine and noradrenaline (76). Dysfunction of these neurotransmitters and their receptors is known to result in mood disorders like anxiety (77). A further study with more focus towards signaling of neurotransmitters is warranted to further unravel underlying mechanisms of CNP-induced anxiety.

One unanticipated finding was that no differences were found in the open field behavior of prenatally exposed mice. Hougaard *et al.*, for instance, found a significant aversion for the open field in C57BL/6 mice prenatally exposed to diesel exhaust particles (19 mg/m^3, GD 9-19, 1 h/day) (78). Similar findings were shown for prenatal inhaled exposure to UV-Titan L181 nanoparticles (42 mg/m^3, GD 9-18, 1 h/day) (79). On the other hand, almost the contrary has been observed in NMRI mice gestationally exposed to CB (4.6 mg/m^3, GD 4-15, 45 min/day), which spent significantly longer time in the central zone (80). This finding has also been supported by a recent study with C57BL/6 mice prenatally exposed to PM via nasal drips (3 mg/kg body weight, embryonic days 2.5, 5.5, 8.5, 11.5, 14.5, and 17.5), showing higher tendencies to visit the center (81).

There are several explanations why all these and the current study are contradictive. First of all, timing of the exposure differed between the studies above. In this context, Umezawa *et al.* argued that initiation of exposure as early as at GD 4 may have interfered with the epigenetic reprogramming prior to implantation, and the formation of PVM neurons and astrocytes in the fetal brain (80, 82). If behavioral changes arose due to disturbances this early in the development, it might be that later gestational exposures were too late for the pattern to signify. However, this still provides no explanation for the observations made here, as exposure in the current study already began at GD 3. Other explanations might be the usage of the various particle types, dosages and administration routes. As explained earlier, the physicochemical properties of particulates in general play a key role in their mode of actions (83). All studies above used a particulate either differing chemically or by size and shape. It could be that this significantly affected their particle toxicity. Moreover, the CNPs that we used were almost free of impurities, while outdoor PM has many other toxic chemical compounds attached to its surface contributing to toxicity. Besides, intratracheal installation and nasal drips are known for their different particle toxicity, because compared to inhalation, they lead to a higher deposition inside the lungs and brains, respectively (84). Lastly, the studies above generally employed much higher doses, rendering it more likely to observe negative or altered behavioral effects. However, it should be noted that these arguments remain speculative and further research is required to elucidate this. days 2.5, 5.5,

8.5, 11.5, 14.5, and 17.5), showing higher tendencies to visit the center (81).

In the homing test, we were unable to observe altered behavior, suggesting that the olfactory performance of the mice remained intact. Nonetheless, it has been postulated by previous research that air pollution can trigger hyposmia (i.e., reduced ability to detect odors). Hyposmia is typically manifested by the loss of olfactory sensory neurons in the olfactory bulb (85), the brain area that is primarily targeted following inhalation of PM through the nasal route. A case-control study with participants diagnosed with hyposmia, for instance, found an association between long-term exposure to $PM_{2.5}$ and olfactory dysfunction (86). Similar findings were observed in animal studies. A recent publication by Hernandez *et al.*, for instance, indicated neurological injury and olfaction latency in mice intranasally exposed to PM over longer term (87). These results do not support the findings reported here. However, it was not hypothesized that the current exposure would already have implications for olfaction, as olfactory dysfunction is mainly known to occur after chronic exposures, in elderly, and more severe neurodegenerative diseases, such as Parkinson's (33, 88).

In the present study, we used GFAP (glial fibrillary acidic protein) and IBA-1 (Ionized calcium-Binding Adapter molecule 1) as markers to detect glial cell activation. However, since the data could not be statistically analyzed, it can only provide a glimpse into the potential mechanisms underlying the early-life exposure. In a healthy brain, microglial activation is only temporary until the disturbance is over (89). However, if clearance fails or the exposure is chronic, microglial cells may induce neuronal death (90, 91). Primary mouse microglial cells exposed to diesel exhaust particles ($PM_{2.5}$) produced, for instance, increased amounts of pro-inflammatory cytokines (e.g. Interleukin 1-β and 6), as well as increased reactive oxygen species (ROS) production (92, 93). Similar observations were shown in primary rat microglia exposed to UFPs after both an acute (<24h) and chronic (<7d) exposure treatment (94). In a study with rats prenatally exposed to traffic-related PM, several brain areas showed significant increase in IBA-1 staining, a marker for microglia activation (95). Almost simultaneously or at least immediately after microglia activation, astrocytes are stimulated to release oxidant species and pro-inflammatory cytokines enhancing neurotoxicity. Increased glial GFAP levels, indicating astrocyte activation and gliosis (96), have been documented in the brains, both in adult and neonatal rodents after $PM_{2.5}$ exposure (97). Furthermore, prenatal and early postnatal exposure to UFPs have been shown to induce astrocyte activation link to depression and autism-like behavior in adult rodents (98). This data points towards the importance of studies exploring the mediating role of glial cells in neuroinflammation and consequent effects on neurodevelopment by early-life exposure to PM.

Early-life exposure did not result in a disturbed behavioral development, or at least no differences were detected in righting, negative geotaxis and cliff aversion. These tests are often employed to investigate early complications of CNS disease and neurodevelopmental disorders, such as autism. However, to our knowledge, this was one of the first studies using these tests to assess the impact of early-life PM on neurodevelopment. Consequently, it is very challenging to interpret these findings as no comparisons are available. One of the neurological responses assessed was the vestibular system of the inner ear. Interestingly, a recent South Korean study found that Meniere's disease risk was significantly correlated with various air pollutants, including PM_{10} (12). Besides, a substantial body of evidence is available that provides links between early-life PM and neurodevelopmental disorders in childhood or later in adulthood. It has, for instance, been found that exposures to PM_1 during the first 3 years of life, are associated with increased risk of autism spectrum disorders (99). Similarly as in humans, Sprague-Dawley rats exposed to $PM_{2.5}$ in the early-postnatal period, displayed typical behavioral features of autism, including poor social interaction, novelty avoidance, and communication deficits (100). Interestingly, they also found the microglia and astrocytes to be activated in the rat brains, further supporting the link discussed earlier of glial activation to neurodevelopmental defects. Next to autism, exposure to $PM_{2.5}$ during childhood is associated with an increased risk of Attention-Deficit/Hyperactivity Disorder (ADHD), as suggested by a Danish cohort study (101)In our study, we did not observe such behavioral developmental deficits. A possible explanation is the limited number of tests included. However, we only included behavioral developmental data of 1

day at PND16. This potentially led to 2 major implications. First, most developmental responses in rodents appear already within the first 10 days of life. To detect a potential delay, it would thus have been better to test the mice on the days that the appearance of the response was expected. However, it was not possible to perform the tests those days due to the exposures taking place. Second, we only included one measurement, at PND 16, while an additional trial would have allowed comparison of the developmental responses over time.

This study has several strengths worth mentioning. First of all, our established white-light detection method has multiple advantages over conventionally employed techniques (e.g., light and electron microscopy). While these methods often require laborious and extensive sample preparation, here, particles can be imaged in tissues almost immediately after sectioning without labelling. Besides, this technique allows detection of particles in a specific and highly sensitive way, with a high detection limit sufficient to measure low doses. Second, we were able to gain insights into the effective dosage delivered in a personalized way, enabling a better estimation of the extent of particle transfer. The lack of dosage characterization is a common limitation in many inhalation studies that solely rely on their delivered exposure concentration to interpret their findings. Third, we applied a concentration of particles that is proportional to concentrations we humans inhale daily, for instance, in a traffic tunnel. This renders the exposure more realistic than many of the studies mentioned above that employed very high concentrations. Lastly, we exposed the mice on days of pregnancy and neonatal life that are particularly crucial for neurodevelopment, allowing us to assess the causal link between the exposure and observed effects.

However, also several limitations need to be acknowledged. First of all, it cannot be guaranteed that all particles found in the brains of offspring solely originated from the delivered exposure. This uncertainty stems from the practical reason that mice were exposed to ambient room air during handling and the behavioral experiments. Albeit the exposure to particles from room air was negligibly small compared to the administered exposure in the inhalation unit, total elimination of ambient exposure was not possible. Another limitation lies in the fact that for this study, the offspring's behavior was only evaluated at one time point, rendering it challenging to detect potential neurodevelopmental delay. Besides, as mentioned earlier, most developmental reflexes already develop during the first 10 days of the mouse's lifetime, while here behavioral development was examined at the age of 16 days. Therefore, mice were probably already past this developmental stage. Lastly, some of the results were subject to very low sample sizes (e.g. staining of GFAP and IBA-1) and consequently, caution must be applied with interpretation. In summary, this research has thrown up many new questions in need of further investigation. Further research on long-term effects in the adult life of mice is warranted to gain a comprehensive understanding of the lifelong effects of perinatal exposure to CNPs.

CONCLUSION

In summary, our work reveals that airborne CNPs, a surrogate of outdoor ultrafine PM, have the ability to deposit within the developing brains following maternal and early-postnatal whole-body exposure. Moreover, we detected altered offspring behavior in the open field test indicative of anxiety-like behavior, and staining of GFAP and IBA-1 provided indications of glial cell activation. An assessment of early behavioral development and olfactory performance did not reveal any exposure-related effects. However, the combination of findings provides support for the hypothesis that early-life exposure to CNPs results in developmental neurotoxicity, which may have complications for the central nervous system later in life. The present data will aid future investigations examining the potential effects and features of nanoparticle-based toxicity. Moreover, this research can contribute to the adoption of protective strategies against occupational and unintended exposure to CNPs.

REFERENCES

1. World Health Organization: Public health and environment [updated 20222022 26 Mar]. Available from: https://www.who.int/data/gho/data/themes/public-health-and-environment.
2. Mannucci PM, Harari S, Martinelli I, Franchini M. Effects on health of air pollution: a narrative review. Intern Emerg Med. 2015;10(6):657-62.
3. World Health Organization. Health topics: Air pollution [updated 20222022 26 Mar]. Available from: https://www.who.int/health-topics/air-pollution#tab=tab_1.
4. Faustini A, Stafoggia M, Colais P, Berti G, Bisanti L, Cadum E, et al. Air pollution and multiple acute respiratory outcomes. Eur Respir J. 2013;42(2):304-13.
5. Liu S, Lim YH, Chen J, Strak M, Wolf K, Weinmayr G, et al. Long-term Air Pollution Exposure and Pneumonia Related Mortality in a Large Pooled European Cohort. Am J Respir Crit Care Med. 2022.
6. Hayes RB, Lim C, Zhang Y, Cromar K, Shao Y, Reynolds HR, et al. PM2.5 air pollution and cause-specific cardiovascular disease mortality. Int J Epidemiol. 2020;49(1):25-35.
7. Verhoeven JI, Allach Y, Vaartjes ICH, Klijn CJM, de Leeuw FE. Ambient air pollution and the risk of ischaemic and haemorrhagic stroke. Lancet Planet Health. 2021;5(8):e542-e52.
8. Monks PS, Granier C, Fuzzi S, Stohl A, Williams ML, Akimoto H, et al. Atmospheric composition change – global and regional air quality. Atmospheric Environment. 2009;43(33):5268-350.
9. IrCELine: What is particulate matter composed of? [updated 20222022 26 Mar]. Available from: https://www.irceline.be/en/documentation/faq/what-is-particulate-matter-composed-of.
10. Ning Z, Sioutas C. Atmospheric Processes Influencing Aerosols Generated by Combustion and the Inference of Their Impact on Public Exposure: A Review. Aerosol and Air Quality Research. 2010;10(1):43-58.
11. Wyzga RE, Rohr AC. Long-term particulate matter exposure: Attributing health effects to individual PM components. Journal of the Air & Waste Management Association. 2015;65(5):523-43.
12. Dong J, Shang Y, Tian L, Inthavong K, Qiu D, Tu J. Ultrafine particle deposition in a realistic human airway at multiple inhalation scenarios. International Journal for Numerical Methods in Biomedical Engineering. 2019;35:e3215.
13. Clifford S, Mazaheri M, Salimi F, Ezz WN, Yeganeh B, Low-Choy S, et al. Effects of exposure to ambient ultrafine particles on respiratory health and systemic inflammation in children. Environ Int. 2018;114:167-80.
14. Schraufnagel DE. The health effects of ultrafine particles. Experimental & Molecular Medicine. 2020;52(3):311-7.
15. Moreno-Ríos AL, Tejeda-Benítez LP, Bustillo-Lecompte CF. Sources, characteristics, toxicity, and control of ultrafine particles: An overview. Geoscience Frontiers. 2022;13(1):101147.
16. Oberdörster G, Oberdörster E, Oberdörster J. Nanotoxicology: an emerging discipline evolving from studies of ultrafine particles. Environ Health Perspect. 2005;113(7):823-39.
17. Ning Z, Geller MD, Moore KF, Sheesley R, Schauer JJ, Sioutas C. Daily Variation in Chemical Characteristics of Urban Ultrafine Aerosols and Inference of Their Sources. Environmental Science & Technology. 2007;41(17):6000-6.
18. Kreyling WG, Semmler-Behnke M, Seitz J, Scymczak W, Wenk A, Mayer P, et al. Size dependence of the translocation of inhaled iridium and carbon nanoparticle aggregates from the lung of rats to the blood and secondary target organs. Inhal Toxicol. 2009;21 Suppl 1:55-60.
19. Peters A, Veronesi B, Calderón-Garcidueñas L, Gehr P, Chen LC, Geiser M, et al. Translocation and potential neurological effects of fine and ultrafine particles a critical update. Particle and Fibre Toxicology. 2006;3(1):13.
20. Calderón-Garcidueñas L, Solt AC, Henríquez-Roldán C, Torres-Jardón R, Nuse B, Herritt L, et al. Long-term air pollution exposure is associated with neuroinflammation, an altered innate immune response, disruption of the blood-brain barrier, ultrafine particulate deposition, and accumulation of amyloid beta-42 and alpha-synuclein in children and young adults. Toxicol Pathol. 2008;36(2):289-310.
21. Lucchini RG, Dorman DC, Elder A, Veronesi B. Neurological impacts from inhalation

of pollutants and the nose-brain connection. Neurotoxicology. 2012;33(4):838-41.
22. Oberdörster G, Sharp Z, Atudorei V, Elder A, Gelein R, Kreyling W, et al. Translocation of inhaled ultrafine particles to the brain. Inhal Toxicol. 2004;16(6-7):437-45.
23. Babadjouni RM, Hodis DM, Radwanski R, Durazo R, Patel A, Liu Q, et al. Clinical effects of air pollution on the central nervous system; a review. J Clin Neurosci. 2017;43:16-24.
24. Shi L, Wu X, Danesh Yazdi M, Braun D, Abu Awad Y, Wei Y, et al. Long-term effects of PM(2·5) on neurological disorders in the American Medicare population: a longitudinal cohort study. Lancet Planet Health. 2020;4(12):e557-e65.
25. Tonne C, Elbaz A, Beevers S, Singh-Manoux A. Traffic-related air pollution in relation to cognitive function in older adults. Epidemiology. 2014;25(5):674-81.
26. Ranft U, Schikowski T, Sugiri D, Krutmann J, Krämer U. Long-term exposure to traffic-related particulate matter impairs cognitive function in the elderly. Environ Res. 2009;109(8):1004-11.
27. Wu Y, Yin J, Cao W, Kang H, Song Q, Bian J, et al. [Effects of fine particulate matter on cognitive function and gut microbiota in adult male mice]. Wei Sheng Yan Jiu. 2021;50(5):821-6.
28. Zeng Y, Lin R, Liu L, Liu Y, Li Y. Ambient air pollution exposure and risk of depression: A systematic review and meta-analysis of observational studies. Psychiatry Res. 2019;276:69-78.
29. Xue T, Guan T, Zheng Y, Geng G, Zhang Q, Yao Y, et al. Long-term PM(2.5) exposure and depressive symptoms in China: A quasi-experimental study. Lancet Reg Health West Pac. 2021;6:100079.
30. Sullivan KJ, Ran X, Wu F, Chang CH, Sharma R, Jacobsen E, et al. Ambient fine particulate matter exposure and incident mild cognitive impairment and dementia. J Am Geriatr Soc. 2021;69(8):2185-94.
31. Rhew SH, Kravchenko J, Lyerly HK. Exposure to low-dose ambient fine particulate matter PM2.5 and Alzheimer's disease, non-Alzheimer's dementia, and Parkinson's disease in North Carolina. PLoS One. 2021;16(7):e0253253.
32. Shaffer RM, Li G, Adar SD, Dirk Keene C, Latimer CS, Crane PK, et al. Fine Particulate Matter and Markers of Alzheimer's Disease Neuropathology at Autopsy in a Community-Based Cohort. J Alzheimers Dis. 2021;79(4):1761-73.
33. Ritz B, Lee PC, Hansen J, Lassen CF, Ketzel M, Sørensen M, et al. Traffic-Related Air Pollution and Parkinson's Disease in Denmark: A Case-Control Study. Environ Health Perspect. 2016;124(3):351-6.
34. Roux J, Bard D, Le Pabic E, Segala C, Reis J, Ongagna JC, et al. Air pollution by particulate matter PM(10) may trigger multiple sclerosis relapses. Environ Res. 2017;156:404-10.
35. Matson U, Ekberg L, Afshari A. Measurement of Ultrafine Particles: A Comparison of Two Handheld Condensation Particle Counters. Aerosol Science and Technology - AEROSOL SCI TECH. 2004;38:487-95.
36. Kumar P, Robins A, Vardoulakis S, Quincey P. Technical challenges in tackling regulatory concerns for urban atmospheric nanoparticles. Particuology. 2011;9(6):566-71.
37. Au WW. Susceptibility of children to environmental toxic substances. Int J Hyg Environ Health. 2002;205(6):501-3.
38. Wang Q, Benmarhnia T, Zhang H, Knibbs LD, Sheridan P, Li C, et al. Identifying windows of susceptibility for maternal exposure to ambient air pollution and preterm birth. Environ Int. 2018;121(Pt 1):317-24.
39. Gong X, Lin Y, Bell ML, Zhan FB. Associations between maternal residential proximity to air emissions from industrial facilities and low birth weight in Texas, USA. Environ Int. 2018;120:181-98.
40. Soma-Pillay P, Nelson-Piercy C, Tolppanen H, Mebazaa A. Physiological changes in pregnancy. Cardiovasc J Afr. 2016;27(2):89-94.
41. Klepac P, Locatelli I, Korošec S, Künzli N, Kukec A. Ambient air pollution and pregnancy outcomes: A comprehensive review and identification of environmental public health challenges. Environ Res. 2018;167:144-59.
42. Basha S, Surendran N, Pichichero M. Immune responses in neonates. Expert Review of Clinical Immunology. 2014;10(9):1171-84.
43. Chiu YH, Hsu HH, Coull BA, Bellinger DC, Kloog I, Schwartz J, et al. Prenatal particulate air pollution and neurodevelopment in urban children: Examining sensitive windows and sex-specific associations. Environ Int. 2016;87:56-65.
44. Costa LG, Cole TB, Dao K, Chang Y-C, Garrick JM. Developmental impact of air pollution

on brain function. Neurochemistry International. 2019;131:104580.
45. Zheng X, Wang X, Wang T, Zhang H, Wu H, Zhang C, et al. Gestational Exposure to Particulate Matter 2.5 (PM2.5) Leads to Spatial Memory Dysfunction and Neurodevelopmental Impairment in Hippocampus of Mice Offspring. Frontiers in Neuroscience. 2019;12.
46. Basagaña X, Esnaola M, Rivas I, Amato F, Alvarez-Pedrerol M, Forns J, et al. Neurodevelopmental Deceleration by Urban Fine Particles from Different Emission Sources: A Longitudinal Observational Study. Environ Health Perspect. 2016;124(10):1630-6.
47. Morris-Schaffer K, Merrill A, Jew K, Wong C, Conrad K, Harvey K, et al. Effects of neonatal inhalation exposure to ultrafine carbon particles on pathology and behavioral outcomes in C57BL/6J mice. Part Fibre Toxicol. 2019;16(1):10.
48. Li X, Zhang Y, Li B, Yang H, Cui J, Li X, et al. Activation of NLRP3 in microglia exacerbates diesel exhaust particles-induced impairment in learning and memory in mice. Environ Int. 2020;136:105487.
49. Chiu YH, Bellinger DC, Coull BA, Anderson S, Barber R, Wright RO, et al. Associations between traffic-related black carbon exposure and attention in a prospective birth cohort of urban children. Environ Health Perspect. 2013;121(7):859-64.
50. Harris MH, Gold DR, Rifas-Shiman SL, Melly SJ, Zanobetti A, Coull BA, et al. Prenatal and childhood traffic-related air pollution exposure and childhood executive function and behavior. Neurotoxicol Teratol. 2016;57:60-70.
51. Wen Y, Ding X, Guan Q, Hu W, Wang B, Hu Q, et al. Effects of exposure to urban particulate matter SRM 1648a during pregnancy on the neurobehavioral development of offspring mice. Ecotoxicology and Environmental Safety. 2021;215:112142.
52. Davis DA, Bortolato M, Godar SC, Sander TK, Iwata N, Pakbin P, et al. Prenatal exposure to urban air nanoparticles in mice causes altered neuronal differentiation and depression-like responses. PLoS One. 2013;8(5):e64128.
53. Bové H, Bongaerts E, Slenders E, Bijnens EM, Saenen ND, Gyselaers W, et al. Ambient black carbon particles reach the fetal side of human placenta. Nature Communications. 2019;10(1):3866.
54. Arima Y, Fukuoka H. Developmental origins of health and disease theory in cardiology. J Cardiol. 2020;76(1):14-7.
55. Chew S, Lampinen R, Saveleva L, Korhonen P, Mikhailov N, Grubman A, et al. Urban air particulate matter induces mitochondrial dysfunction in human olfactory mucosal cells. Particle and Fibre Toxicology. 2020;17(1):18.
56. Zhang M, Wang Y, Wong RMS, Yung KKL, Li R. Fine particulate matter induces endoplasmic reticulum stress-mediated apoptosis in human SH-SY5Y cells. NeuroToxicology. 2022;88:187-95.
57. Topinka J, Binková B, Mracková G, Stávková Z, Benes I, Dejmek J, et al. DNA adducts in human placenta as related to air pollution and to GSTM1 genotype. Mutat Res. 1997;390(1-2):59-68.
58. Hartz AM, Bauer B, Block ML, Hong JS, Miller DS. Diesel exhaust particles induce oxidative stress, proinflammatory signaling, and P-glycoprotein up-regulation at the blood-brain barrier. Faseb j. 2008;22(8):2723-33.
59. Wang Y, Xiong L, Tang M. Toxicity of inhaled particulate matter on the central nervous system: neuroinflammation, neuropsychological effects and neurodegenerative disease. J Appl Toxicol. 2017;37(6):644-67.
60. Gómez-Budia M, Konttinen H, Saveleva L, Korhonen P, Jalava PI, Kanninen KM, et al. Glial smog: Interplay between air pollution and astrocyte-microglia interactions. Neurochemistry International. 2020;136:104715.
61. Jäkel S, Dimou L. Glial Cells and Their Function in the Adult Brain: A Journey through the History of Their Ablation. Front Cell Neurosci. 2017;11:24.
62. Yang QQ, Zhou JW. Neuroinflammation in the central nervous system: Symphony of glial cells. Glia. 2019;67(6):1017-35.
63. BéruBé K, Balharry D, Sexton K, Koshy L, Jones T. Combustion-derived nanoparticles: mechanisms of pulmonary toxicity. Clin Exp Pharmacol Physiol. 2007;34(10):1044-50.
64. Skovmand A, Jensen A, Maurice C, Marchetti F, Lauvås A, Koponen I, et al. Effects of maternal inhalation of carbon black nanoparticles on reproductive and fertility parameters in a four-generation study of male mice. Particle and Fibre Toxicology. 2019;16:13.

65. Bové H, Steuwe C, Fron E, Slenders E, D'Haen J, Fujita Y, et al. Biocompatible Label-Free Detection of Carbon Black Particles by Femtosecond Pulsed Laser Microscopy. Nano Letters. 2016;16(5):3173-8.
66. Fournier SB, D'Errico JN, Adler DS, Kollontzi S, Goedken MJ, Fabris L, et al. Nanopolystyrene translocation and fetal deposition after acute lung exposure during late-stage pregnancy. Particle and Fibre Toxicology. 2020;17(1):55.
67. Calderón-Garcidueñas L, Pérez-Calatayud Á A, González-Maciel A, Reynoso-Robles R, Silva-Pereyra HG, Ramos-Morales A, et al. Environmental Nanoparticles Reach Human Fetal Brains. Biomedicines. 2022;10(2).
68. Hameed S, Zhao J, Zare RN. Ambient PM particles reach mouse brain, generate ultrastructural hallmarks of neuroinflammation, and stimulate amyloid deposition, tangles, and plaque formation. Talanta Open. 2020;2:100013.
69. Walz N, Mühlberger A, Pauli P. A Human Open Field Test Reveals Thigmotaxis Related to Agoraphobic Fear. Biological Psychiatry. 2016;80(5):390-7.
70. Liu J, Yang C, Yang J, Song X, Han W, Xie M, et al. Effects of early postnatal exposure to fine particulate matter on emotional and cognitive development and structural synaptic plasticity in immature and mature rats. Brain Behav. 2019;9(12):e01453-e.
71. Yolton K, Khoury JC, Burkle J, LeMasters G, Cecil K, Ryan P. lifetime exposure to traffic-related air pollution and symptoms of depression and anxiety at age 12 years. Environ Res. 2019;173:199-206.
72. Ng F, Berk M, Dean O, Bush AI. Oxidative stress in psychiatric disorders: evidence base and therapeutic implications. Int J Neuropsychopharmacol. 2008;11(6):851-76.
73. de Oliveira MR, Silvestrin RB, Mello EST, Moreira JC. Oxidative stress in the hippocampus, anxiety-like behavior and decreased locomotory and exploratory activity of adult rats: effects of sub acute vitamin A supplementation at therapeutic doses. Neurotoxicology. 2007;28(6):1191-9.
74. Salim S, Asghar M, Chugh G, Taneja M, Xia Z, Saha K. Oxidative stress: a potential recipe for anxiety, hypertension and insulin resistance. Brain Res. 2010;1359:178-85.
75. Morris RH, Counsell SJ, McGonnell IM, Thornton C. Early life exposure to air pollution impacts neuronal and glial cell function leading to impaired neurodevelopment. Bioessays. 2021;43(9):e2000288.
76. Suzuki T, Oshio S, Iwata M, Saburi H, Odagiri T, Udagawa T, et al. In utero exposure to a low concentration of diesel exhaust affects spontaneous locomotor activity and monoaminergic system in male mice. Particle and Fibre Toxicology. 2010;7(1):7.
77. Martin EI, Ressler KJ, Binder E, Nemeroff CB. The neurobiology of anxiety disorders: brain imaging, genetics, and psychoneuroendocrinology. Psychiatr Clin North Am. 2009;32(3):549-75.
78. Hougaard KS, Jensen KA, Nordly P, Taxvig C, Vogel U, Saber AT, et al. Effects of prenatal exposure to diesel exhaust particles on postnatal development, behavior, genotoxicity and inflammation in mice. Particle and Fibre Toxicology. 2008;5(1):3.
79. Hougaard KS, Jackson P, Jensen KA, Sloth JJ, Löschner K, Larsen EH, et al. Effects of prenatal exposure to surface-coated nanosized titanium dioxide (UV-Titan). A study in mice. Part Fibre Toxicol. 2010;7:16.
80. Umezawa M, Onoda A, Korshunova I, Jensen ACØ, Koponen IK, Jensen KA, et al. Maternal inhalation of carbon black nanoparticles induces neurodevelopmental changes in mouse offspring. Particle and Fibre Toxicology. 2018;15(1):36.
81. Li S, Liu Y, Liu B, Hu Y-Q, Ding Y-Q, Zhang J, et al. Maternal urban particulate matter exposure and signaling pathways in fetal brains and neurobehavioral development in offspring. Toxicology. 2022;474:153225.
82. Kafri T, Ariel M, Brandeis M, Shemer R, Urven L, McCarrey J, et al. Developmental pattern of gene-specific DNA methylation in the mouse embryo and germ line. Genes Dev. 1992;6(5):705-14.
83. Luyts K, Napierska D, Nemery B, Hoet P. How physico-chemical characteristics of nanoparticles cause their toxicity: Complex and unresolved interrelations. Environmental Science-Processes & Impacts. 2013;15:23-38.
84. Osier M, Oberdörster G. Intratracheal inhalation vs intratracheal instillation: differences in particle effects. Fundam Appl Toxicol. 1997;40(2):220-7.

85. Vent J, Robinson AM, Gentry-Nielsen MJ, Conley DB, Hallworth R, Leopold DA, et al. Pathology of the olfactory epithelium: smoking and ethanol exposure. Laryngoscope. 2004;114(8):1383-8.
86. Zhang Z, Rowan NR, Pinto JM, London NR, Lane AP, Biswal S, et al. Exposure to Particulate Matter Air Pollution and Anosmia. JAMA Netw Open. 2021;4(5):e2111606.
87. Hernandez M, Vaughan J, Gordon T, Lippmann M, Gandy S, Chen LC. World Trade Center dust induces nasal and neurological tissue injury while propagating reduced olfaction capabilities and increased anxiety behaviors. Inhal Toxicol. 2022:1-14.
88. Ajmani GS, Suh HH, Pinto JM. Effects of Ambient Air Pollution Exposure on Olfaction: A Review. Environmental health perspectives. 2016;124(11):1683-93.
89. Kettenmann H, Hanisch UK, Noda M, Verkhratsky A. Physiology of microglia. Physiol Rev. 2011;91(2):461-553.
90. Genc S, Zadeoglulari Z, Fuss SH, Genc K. The adverse effects of air pollution on the nervous system. J Toxicol. 2012;2012:782462.
91. Tang Y, Le W. Differential Roles of M1 and M2 Microglia in Neurodegenerative Diseases. Mol Neurobiol. 2016;53(2):1181-94.
92. Harry GJ, Kraft AD. Microglia in the developing brain: a potential target with lifetime effects. Neurotoxicology. 2012;33(2):191-206.
93. Roqué PJ, Dao K, Costa LG. Microglia mediate diesel exhaust particle-induced cerebellar neuronal toxicity through neuroinflammatory mechanisms. Neurotoxicology. 2016;56:204-14.
94. Levesque S, Taetzsch T, Lull ME, Kodavanti U, Stadler K, Wagner A, et al. Diesel exhaust activates and primes microglia: air pollution, neuroinflammation, and regulation of dopaminergic neurotoxicity. Environ Health Perspect. 2011;119(8):1149-55.
95. Woodward NC, Haghani A, Johnson RG, Hsu TM, Saffari A, Sioutas C, et al. Prenatal and early life exposure to air pollution induced hippocampal vascular leakage and impaired neurogenesis in association with behavioral deficits. Translational Psychiatry. 2018;8(1):261.
96. Eng LF, Ghirnikar RS, Lee YL. Glial fibrillary acidic protein: GFAP-thirty-one years (1969-2000). Neurochem Res. 2000;25(9-10):1439-51.
97. Xu MX, Zhu YF, Chang HF, Liang Y. Nanoceria restrains PM2.5-induced metabolic disorder and hypothalamus inflammation by inhibition of astrocytes activation related NF-κB pathway in Nrf2 deficient mice. Free Radic Biol Med. 2016;99:259-72.
98. Haghani A, Johnson R, Safi N, Zhang H, Thorwald M, Mousavi A, et al. Toxicity of urban air pollution particulate matter in developing and adult mouse brain: Comparison of total and filter-eluted nanoparticles. Environment International. 2020;136:105510.
99. Chen B, Huang S, He J, He Q, Chen S, Liu X, et al. Sex-specific influence of prenatal air pollutant exposure on neonatal neurobehavioral development and the sensitive window. Chemosphere. 2020;254:126824.
100. Volk HE, Lurmann F, Penfold B, Hertz-Picciotto I, McConnell R. Traffic-related air pollution, particulate matter, and autism. JAMA Psychiatry. 2013;70(1):71-7.
101. Thygesen M, Holst GJ, Hansen B, Geels C, Kalkbrenner A, Schendel D, et al. Exposure to air pollution in early childhood and the association with Attention-Deficit Hyperactivity Disorder. Environ Res. 2020;183:108930.

Acknowledgements – First of all, I would like to thank my promotor, prof. Dr. Michelle Plusquin, for this wonderful opportunity to do my internship at the Environmental Biology research group. Next, I would like to greatly acknowledge my supervisors, Mr. Kenneth Vanbrabant and Ms. Leen Rasking. Thank you, Ms. Rasking, for providing so much additional support throughout the internship! The feedback during the writing process was very helpful. Lastly, I would like to thank Mr. Kenneth Vanbrabant in particular, for the incredible support and opportunities I got throughout the entire process. I had the chance to grow as a scientist and person, and found my way through it to become a researcher myself. I am grateful for that!

Author contributions – MP and KV conceived and designed the research. KV and MV performed experiments and data analysis. LR provided assistance with behavioral testing. MV wrote the paper. All authors carefully edited the manuscript.

SUPPLEMENTARY INFORMATION

S1: Exposure characterization and monitoring – The generated particles had an foreseen primary size of 1-20 nm and negligibly small levels of impurities. Mass-concentrations of total suspended particles were monitored gravimetrically by sampling on filters (PTFE Membrane filters, Fisher Scientific Co., USA). Exposure air was sampled twice for 220 min at an airflow of 5 L/min, and weighted using a Tapered Element Oscillating Microbalance. Particle number and mobility particle size distributions of the control and exposure atmosphere were measured using a Scanning Mobility Particle Sizer™ Spectrometer (SMPS™, TSI Inc., USA). Temperature and relative humidity inside the units were measured every hour; CO_2/O_2 concentrations were measured once a day.

S2: Behavioral developmental tests – For the righting test, pups were placed on their back on the table surface and held immobile for 3 sec. The time required for the pup to right back onto 4 paws was recorded. In the negative geotaxis test, pups were placed face down on an incline of 45° and held immobile for 5 sec. Next, the pup was released and the time and direction to face upward was recorded. Scores were given for this response and included 0 for falling down the incline or failing to turn; 1 for turning the head; 2 for turning the body up 90°; 3 for turning the body up 180°; 4 for climbing up the slope. In the cliff aversion test, the pup is placed on the edge of a surface so that the forepaws are dangling over the edge. Scoring was based on the average time needed to remove the snout and paws from the edge, as well as on predetermined scores. These included 0 for remaining motionless or when it falls from the edge, 1 when it turns the head aside; 2 when it turns the head aside, pulls back the forepaw, and puts them on the surface; 3 when it initiates a backward movement. All tests were repeated thrice, and scores and times were averaged.

S3: Quantification of IBA-1 and GFAP in immunofluorescent stained brain sections – After obtaining the 32 digital images (16 for IBA-1, 16 for GFAP) as described in "Immunofluorescence", the files were opened in Fiji (ImageJ v2.0, Open source software) for further processing. The pixels stained with Alexa Fluor® 488 were quantified, by converting the images to grayscale levels (command, Image: Color: Split Channels). Next, the greyscale threshold was set to 70, so that all pixels above this greyscale were included for the measurements (command, Image: Adjust: Threshold). Using histogram analyses (command, Analyze: Set Measurements) after clicking the settings "Area" and "Limit to threshold", the fraction of white pixels representing the area of expression could be determined. The mean value of immunofluorescence was calculated for each brain sections within each condition.